BILINGUAL PUBLISHING GROUP

Journal of Atmospheric Science Research

https://journals.bilpubgroup.com/index.php/jasr/index

ARTICLE

Changes in Future Rainfall over Southeast Asia Using the CMIP6 Multi-model Ensemble

Bhenjamin Jordan Ona*[*], *Srivatsan V Raghavan*, *Ngoc Son Nguyen*, *Sheau Tieh Ngai*, *Thanh Hung Nguyen

Tropical Marine Science Institute, National University of Singapore, 119227, Singapore

ABSTRACT

A multi-model ensemble from the new CMIP6 models was utilized to determine the future changes in precipitation over Southeast Asia (SEA; longitude: 90°E–140°E, latitude: 15°S–30°N). The changes are computed for the three (3) future time slices (2021–2040, 2041–2060, and 2081–2100) under four (4) different scenarios based on the Shared Socioeconomic Pathways (SSPs): 1-2.6, 2-4.5, 3-7.0, and 5-8.5. Our results indicate that future rainfall in the SEA-averaged region could increase by about 4%, 5%, 6%, and 9% towards the end of the century relative to the present-day average (1995–2014) under SSP1-2.6, 2-4.5, 3-7.0, and 5-8.5, respectively. Among all scenarios, SSP3-7.0 widely shows remarkably dry conditions whereas SSP5-8.5 suggests extremely wet conditions on different time scales. A clear dissociation of wet and dry areas is expected in the far-term period (2081–2100). Changes in the annual cycle indicate that monsoon rainfall could experience significant increases. The study also emphasizes the importance of moisture flux convergence (MFC) in determining precipitation patterns across different seasons and regions. The results suggest that MFC plays a crucial role in the projected increase or decrease of rainfall in SEA regions. Spatial correlation of future global mean temperature (GMT) and rainfall have a high positive (negative) correlation in the north (south) latitudes. Changes in rainfall are found to be sensitive to GMT. The responses to future rainfall changes per degree Celsius of warming are at the rate of 8.9%, 6.3%, 3.6%, and 2.7% under SSP1-2.6, 2-4.5, 3-7.0, and 5-8.5, respectively.

Keywords: CMIP6; Climate change; Moisture flux convergence; GMT; Southeast Asia; Rainfall

*CORRESPONDING AUTHOR:

Bhenjamin Jordan Ona, Tropical Marine Science Institute, National University of Singapore, 119227, Singapore; E-mail: ona.bhen@nus.edu.sg

ARTICLE INFO

Received: 9 April 2024 | Revised: 23 April 2024 | Accepted: 26 April 2024 | Published Online: 30 April 2024

DOI: https://doi.org/10.30564/jasr.v7i2.6335

CITATION

Ona, B.J., Raghavan, S.V., Nguyen, N.S., et al, 2024. Changes in Future Rainfall over Southeast Asia Using the CMIP6 Multi-model Ensemble. Journal of Atmospheric Science Research. 7(2): 62–82. DOI: https://doi.org/10.30564/jasr.v7i2.6335

1. Introduction

Future changes in climate, especially precipitation, remain uncertain in terms of magnitude, let alone the sign of change. To this end, reliable climate projections generated from climate models are of great value for studying climate impacts from regional through to local scales. The Sixth Assessment Report (AR6) from the Intergovernmental Panel on Climate Change [1–3] published a comprehensive assessment of climate change and its impacts and adaptative strategies for effective decision-making evaluated based on the sophisticated and advanced climate models. The new generation of global climate models (GCMs) and the earth system models (ESMs) under the Coupled Model Intercomparison Project Phase 6 (CMIP6) [4] have been studied over the past few years. The current improvements in the CMIP6 models have demonstrated an advanced ability to capture the characteristics of large-scale climate patterns at a global scale such as climate extremes, monsoon and drought [1, 5–8].

Southeast Asia (hereafter, SEA) is one of the most vulnerable regions to climate-related disasters such as floods and droughts due to intensified climate extremes [9–11]. Observational studies have revealed that the trend of rainfall extremes is increasing in SEA region and is linked to the rising global mean temperature anomaly [11]. It has been shown that an increase of 1.5°C to 2°C in global surface temperatures could result in a net reduction of agricultural yields, threatened freshwater ecosystem, high risks in coastal flooding in the context of both rainfall extremes and sea level rise, and extreme droughts over SEA region [12–18]. Some studies have also demonstrated that these impacts are associated with intensified precipitation extremes through altered atmospheric dynamics of moisture content and circulation patterns in the future [19–25].

Limited studies focusing on the future climate of the SEA region have been carried out and there is a greater need for future assessments of climate change from global and regional models. This paper aims to provide some initial assessments to plausible future climate changes in Southeast Asia. In this context, we analyse future climate projections of precipitation in this region using CMIP6 models under four of the Shared Socioeconomic Pathways (SSPs) scenarios, 1-2.6, 2-4.5, 3-7.0 and 5-8.5. This study brings out certain facets of future climate change investigations along with other studies that have performed similar studies elsewhere [26–34]. The paper is organized thus: Section 2 describes the datasets used and the methodology undertaken in this study. Section 3 presents the results of the evaluation of precipitation changes in the future. Section 4 provides some discussions before drawing some conclusions/recommendations from this study.

2. Methods

2.1 Model data: CMIP6 Ensemble

The CMIP6 is the latest and advanced set of climate models for better understanding of the past, present and future climate of the Earth and detailed documentation is available from Eyring et al. (2016) [4]. The CMIP6 models used in this study are listed in **Table 1**. Here, we assess the future changes in rainfall and its responses to global mean temperature, atmospheric moisture content (water vapour path) of Southeast Asia using the diagnostic outputs generated by the CMIP6 models under four (4) different scenarios based on the Shared Socioeconomic Pathways (SSPs): SSP1-2.6 (sustainability), SSP2-4.5 (middle-of-the-road), SSP3-7.0 (regional rivalry), and SSP5-8.5 (fossil-fueled development), described by O'Neill et al. (2016) [35]. These SSPs represent the future change of greenhouse gas emission and land use scenarios to assess wide range of climate information for application in climate impact modelling, vulnerability assessment, and adaptation. The models used in this study have been taken from a single ensemble member (i.e. r1i1p1f1) for both historical and future experiments. Additional information is available at: https://pcmdi.llnl.gov/CMIP6/ and https://es-doc.org/cmip6-models/ [4].

Table 1. Details of the 48 CMIP6 models used in this study.

No.	Model	Lon. × Lat.	No.	Model	Lon. × Lat.
1	ACCESS-CM2	1.875° × 1.25°	25	GFDL-CM4	1.25° × 1°
2	ACCESS-ESM1-5	1.875° × 1.241°	26	GISS-E2-1-G-CC	2.5° × 2°
3	AWI-ESM-1-1-LR	1.875° × 1.875°	27	GISS-E2-1-G	2.5° × 2°
4	BCC-CSM2-MR	1.25° × 1.125°	28	GISS-E2-1-H	2.5° × 2°
5	BCC-ESM1	2.813° × 2.813°	29	HadGEM3-GC31-LL	1.875° × 1.25°
6	CAMS-CSM1-0	1.125° × 1.125°	30	HadGEM3-GC31-MM	0.833° × 0.556°
7	CAS-ESM2-0	1.406° × 1.406°	31	INM-CM4-8	2° × 1.5°
8	CESM2-FV2	2.5° × 1.875°	32	INM-CM5-0	2° × 1.5°
9	CESM2-WACCM-FV2	2.5° × 1.875°	33	IPSL-CM6A-LR	2.5° × 1.259°
10	CESM2-WACCM	2.5° × 1.875°	34	KACE-1-0-G	1.875° × 1.25°
11	CESM2	2.5° × 1.875°	35	MCM-UA-1-0	3.75° × 2.25°
12	CIESM	1.25° × 1.25°	36	MIROC-ES2L	2.813° × 2.813°
13	CNRM-CM6-1-HR	0.5° × 0.5°	37	MIROC6	1.406° × 1.406°
14	CNRM-CM6-1	1.406° × 1.406°	38	MPI-ESM-1-2-HAM	1.875° × 1.875°
15	CNRM-ESM2-1	1.406° × 1.406°	39	MPI-ESM1-2-HR	0.938° × 0.938°
16	CanESM5-CanOE	2.813° × 2.813°	40	MPI-ESM1-2-LR	1.875° × 1.875°
17	CanESM5	2.813° × 2.813°	41	MRI-ESM2-0	1.25° × 1.25°
18	E3SM-1-0	1° × 1°	42	NESM3	1.875° × 1.875°
19	E3SM-1-1-ECA	1° × 1°	43	NorCPM1	2.5° × 1.875°
20	EC-Earth3-Veg	0.703° × 0.703°	44	NorESM2-LM	2.5° × 1.875°
21	EC-Earth3	0.703° × 0.703°	45	NorESM2-MM	1.25° × 0.938°
22	FGOALS-f3-L	1.25° × 1°	46	SAM0-UNICON	1.25° × 0.938°
23	FGOALS-g3	2° × 2.25°	47	TaiESM1	1.25° × 0.938°
24	FIO-ESM-2-0	1.25° × 0.938°	48	UKESM1-0-LL	1.875° × 1.25°

2.2 Methodology

Monthly precipitation data (mm month^{-1}) from the CMIP6 models were re-gridded onto a 1° × 1° horizontal resolution using bilinear interpolation. We investigated the annual and seasonal precipitation changes across land-only areas of Southeast Asia (SEA; longitude: 90°E–140°E, latitude: 15°S–30°N). We classified the periods of the historical and future simulations into four (4) 20-year time periods: baseline (1995–2014), near-term (2021–2040), mid-term (2041–2060), and far-term (2081–2100). Results for the spatial maps for far-term period are presented in the main paper and for the near- and mid-term in supplementary information **Figure S1** and **Figure S2**. Stippling indicates model agreement in spatial maps (i.e. two-thirds of the models agreed to the sign of change). This dataset is grouped under four seasons to analyze possible seasonal changes in the future: December-January-February (DJF), March-April-May (MAM), June-July-August (JJA), and September-October-November (SON). We subjectively divide the SEA region into three (3) distinct zones based on geographical locations to assess changes in different regions as shown in **Figure 1a**: mainland SEA (D01), the Philippines (D02) and the maritime continent (D03).

We computed the 50th percentile for each grid cell in the spatial and temporal analyses to get the

multi-model median. Where applicable, we computed the 90% confidence intervals to quantify future changes. The 25th to 75th percentile range indicator or the lower to upper interquartile, respectively, was computed to measure the mid-spread (middle 50%) value of the model (as indicated in box plots). In this sense, higher confidence in predictability can be placed among the different models. To establish a direct relationship between warming climate, atmospheric moisture and rainfall, given that these variables could be attributed to the changes in future rainfall, we computed the spatial correlation coefficient for 2021–2099. The sensitivity of future rainfall changes under different scenario to global mean temperature change is discussed.

We also calculated the moisture flux convergence at low-level (850hPa) to describe the transport of atmospheric moisture fluxes which is crucial in influencing precipitation patterns. It refers to the rate at which moisture is converging into a specific location in the atmosphere and is usually quantified as the product of horizontal wind speed and specific humidity gradient. Banacos & Schultz (2005) [36] have provided a detailed explanation of MFC.

The sensitivities of SEA precipitation to global mean temperature (GMT) under various emission scenarios are calculated. This is achieved by determining the change in precipitation in response to incremental increases in global temperature Mathematically, this relationship is expressed as $\Delta Pr = \Delta P/\Delta GMT$, where ΔPr is the responses of precipitation rate, ΔP represents the projected changes in rainfall and ΔGMT denotes the changes in global mean temperature. Such calculations provide insights into the percent changes in precipitation per 1°C of global warming within the CMIP6 dataset across different scenarios. It is noteworthy that according to the Clausius-Clapeyron (C-C) relation, the saturation of global water vapor pressure is expected to increase by approximately 7% for every 1°C rise in global temperature. This fundamental relationship underscores the profound impact that rising temperatures can have on moisture content, which in turn influences precipitation patterns and intensity in regions such as Southeast Asia.

3. Results and discussions

3.1 Annual mean precipitation

The spatial distribution of rainfall of CMIP6 model ensemble for 1995–2014 is illustrated in **Figure 1a**. The analysis reveals distinct patterns in rainfall across different regions, with D03 exhibiting higher rainfall compared to D01 and D02. This is because maritime continent is situated in one of the warmest oceanic regions and serves as a prominent hub for tropical atmospheric convection. Coastal rainfall is seen in the models particularly along Myanmar, Thailand, Indonesia, and the Philippines. The models underscore the significance of factors such as local topography in shaping rainfall patterns.

Figure 1b presents the projections from the CMIP6 models for the 21st century in the Southeast Asia (SEA) region under different scenarios. The analysis reveals an overall increasing trend in rainfall throughout the century across the region. However, there are notable differences in the responses of different scenarios. Specifically, the SSP3-7.0 scenario indicates a drying climate for a significant period until 2085. This suggests that under this particular scenario, the SEA region is projected to experience a decrease in rainfall over the long term. On the other hand, the SSP5-8.5 scenario shows a wetting tendency in the earlier years of the century, indicating an increase in rainfall. Furthermore, SSP5-8.5 exhibits higher increases in rainfall compared to other scenarios, emphasizing its potential for greater changes in precipitation patterns. These projected trends in rainfall under different scenarios highlight the importance of considering different future trajectories of greenhouse gas emissions and socio-economic factors when assessing potential climate outcomes. It is worth noting that these projections are subject to uncertainties associated with climate models and assumptions made in the scenarios.

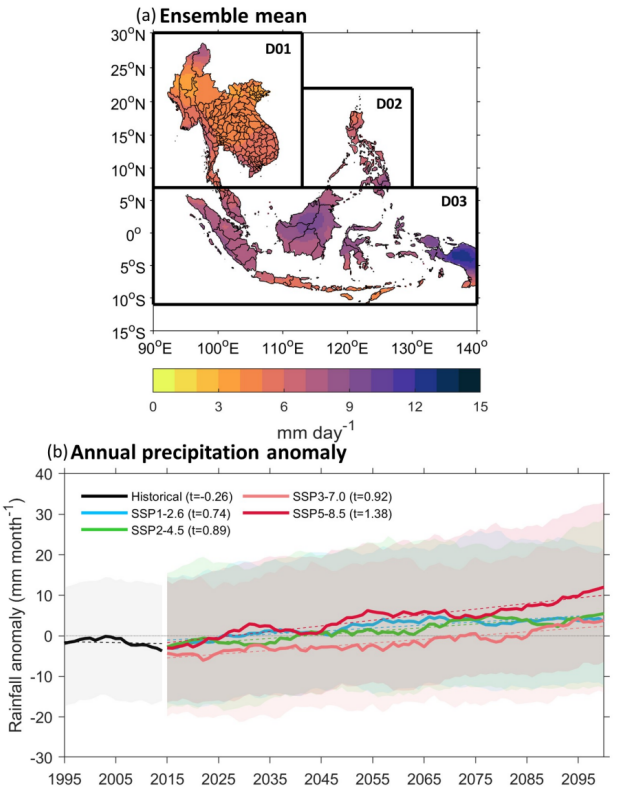

Figure 1. (**a**) Ensemble mean of rainfall from 1995-2014, (**b**) Time series of annual precipitation anomalies (mm month-1; 10 year running mean) relative to the present-day average (1995–2014) for the entire SEA region. Thick black and coloured lines represent the median (50th percentile) of the CMIP6 models for each scenario. Upper and lower boundaries of shaded region are the 75th and the 25th percentiles, respectively. Trend lines are drawn in dashed lines, statistical significance is tested at $p<0.05$.

3.2 Spatial distribution of precipitation changes

Figure 2 displays the annual and seasonal far-term future (2081–2100) changes in precipitation relative to the present-day average (1995–2014), with the stippling indicating a 90% confidence interval. Highest increases and decreases are apparent in the last few decades of the 21st century while relative significant changes are found in the near-term and mid-term period (**Figure S1, S2**). In the near-term (2021–2040) and mid-term (2041–2060) projections, the models depict notable shifts in precipitation patterns across Southeast Asia (SEA) but not as pronounced as in the far-term. For instance, during the annual (ANN) period, a minimal increase in rainfall is projected over most SEA regions except in SSP3-7.0. For far-term, significant changes in precipitation are projected across SEA during the ANN period. Despite reductions in rainfall over certain areas such as Thailand, Myanmar, and Indonesia, there is a noteworthy overall increase in rainfall across most SEA regions. The SSP5-8.5 scenario predicts the highest increases in rainfall, particularly over Myanmar, Kalimantan, and Papua NG. Overall, annual changes reveal substantial increases in rainfall across mainland SEA and parts of Borneo, the Philippines, and Indonesia under all scenarios. However, reduced rainfall is observed over the southern maritime islands of Indonesia. During the DJF period, significant decreases in rainfall are observed over mainland SEA in all scenarios except for SSP 1-2.6.

The DJF season, which is Northwest Monsoon dominated, shows a clear gradient in rainfall patterns – a wetter maritime and a drier mainland. Decrease in rainfall is mostly seen over mainland SEA under high emission scenarios (SSP 3-7.0, 5-8.5) whereas increases in rainfall are seen under the mitigation scenario (SSP 1-2.6). The drier regions are notable over parts of Myanmar, Philippines, Vietnam, and the southern maritime islands of Indonesia. One notable observation among the different scenarios is the SSP 3-7.0, which indicates a predominantly dry near-term future for the entire SEA region. In the near-term period (**Figure S1**), there are minimal increases in rainfall, with projections primarily indicating drying trends over mainland SEA across seasons, except for SON. Subsequently, in the mid-term period (**Figure S1**), this drying tendency becomes more pronounced, particularly evident during the MAM season across SEA.

In the far-term period, the mountainous areas within the maritime continent, mainly, show relatively higher magnitudes of rainfall (again, except SSP3-7.0). During MAM (SON), the analyses on future projections indicated less (more) rainfall over mainland SEA including the Philippines. While most regions in SEA are likely to experience marginally wet changes during SON, the southern part of Indonesia is likely to have reduced precipitation under SSP2-4.5, SSP3-7.0, and SSP5-8.5. The JJA season, during

which the Southwest Monsoon is pronounced, exhibits widespread dry regions of the maritime continent excluding the northern Borneo Island and parts of Peninsular Malaysia. Overall, amongst the different time scales and scenarios, SSP3-7.0 can be considered as a 'dry' scenario.

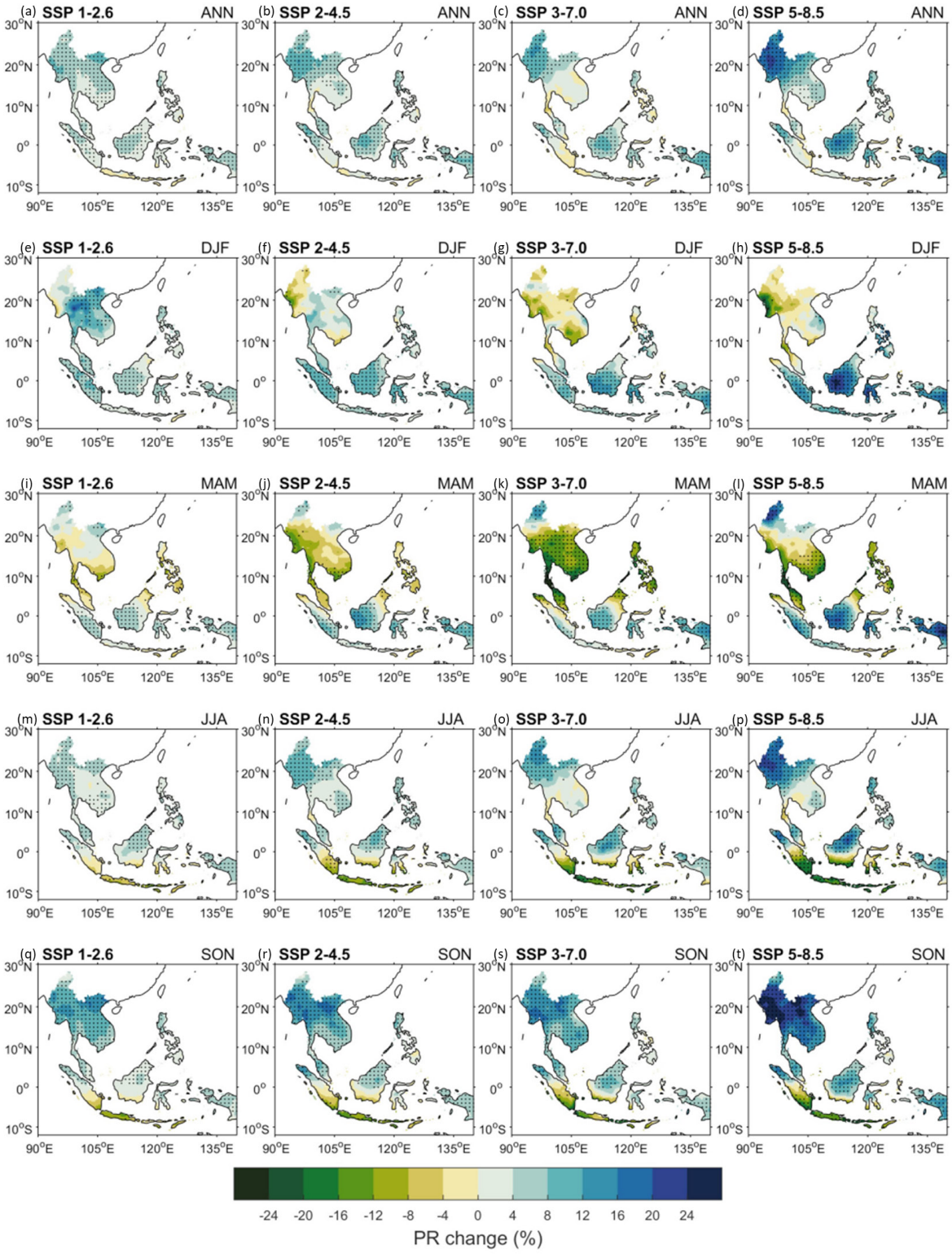

Figure 2. Spatial distribution of (**a–d**) annual and (**e–t**) seasonal precipitation changes for far-term (2081–2100). Stippling indicates that at least two-thirds of the models agree on the sign of changes.

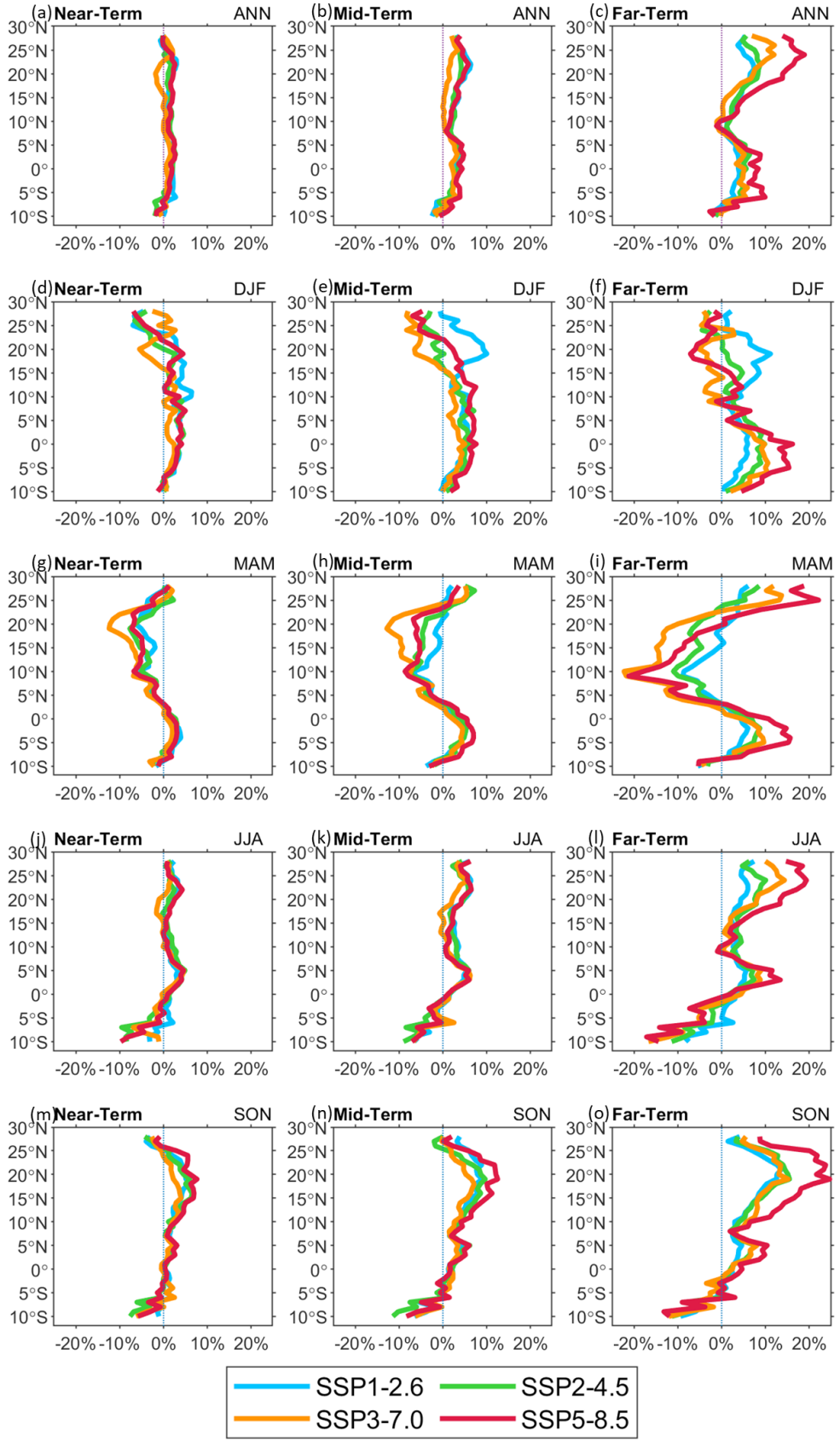

Figure 3. Zonally averaged (**a–c**) annual and (**d–o**) seasonal precipitation change. (X-axis is the precipitation change and Y-axis is the latitude).

Next, we examine the future changes zonally, over the entire SEA region, across time-slices. This is shown in **Figure 3**. While the ANN shows no significant change, DJF shows marginally wetter northern latitudes, except SSP 3.7-0, which shows drier conditions in the near-term period (as reflected in the spatial changes, **Figure 2**). Reduced precipitation can be clearly seen during JJA, in the southern regions of SEA, below the equator. The mid-term shows clear patterns on the changes, with an overall increase on the northern regions above the equator, during ANN. DJF shows larger increases over all regions except decreases under SSPs 2-4.5 and 3.7-0, above 10°N. The JJA season exhibits a clear signal of decrease below the equator while increases above the equator can be seen under all scenarios. The signals of change emerge distinctly during the far-term. The ANN shows minimal decreases over the southern islands below 10°S. DJF shows stronger increases (decreases) of up to 10% and higher over the southern (northern) latitudes, although the increases in the northern latitudes are seen under SSPs 1-2.6 and 2-4.5. Large decreases in precipitation are apparent during MAM and the largest increases are shown during SON from 10°N to 20°N, respectively. JJA changes show a strong dipole with large decreases below the equator and large increases above. The clear patterns of increasing and decreasing rainfall tendencies in the southern (northern) hemispheres of SEA during DJF (JJA), by the end of the century, is probably an indication of an enhanced monsoon precipitation and intensified double-Intertropical Convergence Zone (double-ITCZ). This is not further examined in this study, however, systematic biases of the double-ITCZ were examined by Tian and Dong (2020) [37] and noted a reduction of biases from CMIP5 to CMIP6 models.

3.3 Future changes examined using box plots

Figure 4 summarizes spatially averaged future changes. In the SEA region, the future changes among models indicate a strong median increase up to 4%, 5%, 6% and 9% towards the end of the century under SSP1-2.6, 2-4.5, 3-7.0, and 5-8.5, respectively. The smallest median change is projected under the SSP 3-7.0 during the near- (0.3%) and mid-term (2.4%) periods. Possible extreme changes show a substantial increase of 22% (far-term of SSP 5-8.5) and a decrease of about 8% (near-term of SSP 3-7.0) as represented by the 90th and 10th percentiles, respectively. The continued increase over the different domains in the SEA region in the future is apparent. In D01, D02, and D03, rainfall changes are projected with increases up to 8%, 3.5%, 8%, respectively, during the far-term period.

However, extreme changes are apparently higher in the sub-domains of SEA. Of interest, during the far-term period, upper extreme changes are projected to increase by 33%, 32%, and 22% at the 90th percentile while lower extreme values might decrease by 25%, 30%, 11% at the 10th percentile over D01, D02 and D03, respectively. All the lower extreme changes in the sub-regions are projected under the SSP 3-7.0 whereas the upper extreme changes are exhibited by the SSP 5-8.5. This may be suggestive that under a warmer climate, extreme changes could be exacerbated. It is apparent that a large spread in the interquartile range represents larger uncertainty during the far-term period across all domains.

3.4 Changes in the annual cycle

The multi-model ensemble precipitation annual change is briefly evaluated in **Figure 5**. In the SEA region, future precipitation during December-February shows a strong increase in comparison to other seasons, indicating a likely strengthening of the Northeast Monsoon's influence on rainfall (**Figure 5a**). The months of March-May exhibit the least increase in precipitation in the near-term period. Moreover, the months of June-November show relatively wetter conditions but with a significant increase in the far-term period. The highest change in precipitation is during December with an increase of about 14% under the SSP5-8.5 while May shows a decrease of about 2% during the near-term under SSP3-7.0.

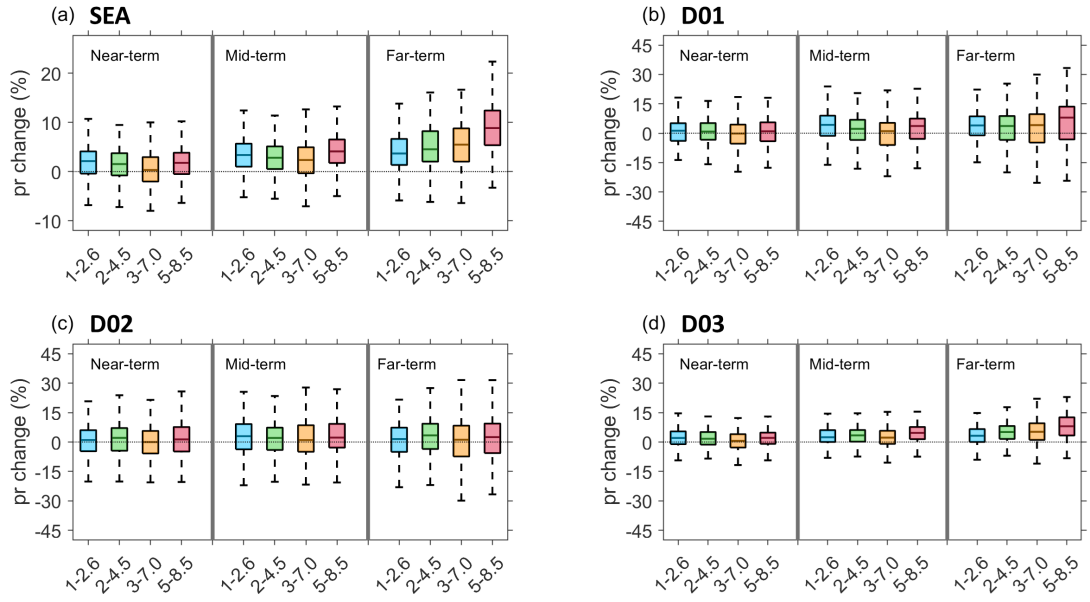

Figure 4. Box plot of the projected precipitation changes for the near-term, mid-term, and long-term relative to the baseline average (1995–2014) in SEA region and in the sub-domains. This shows the 90th (maximum), 75th (upper quartile), 25th (lower quartile), 10th (minimum) percentiles. The center is the 50th percentile or the median of all the models.

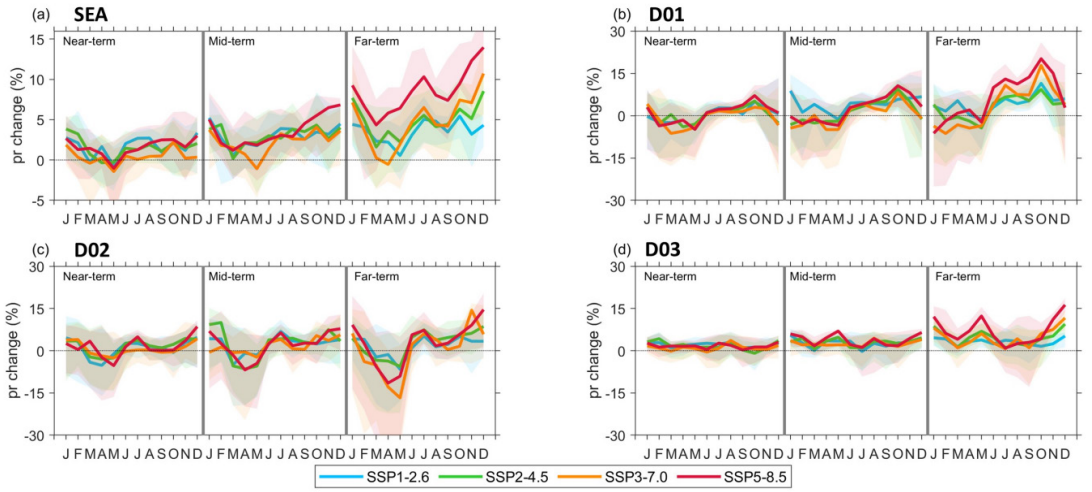

Figure 5. Precipitation changes in the annual cycle. Upper and lower boundaries of the shaded region are the 75th and the 25th percentiles, respectively.

Furthermore, the annual changes display distinct patterns in the different domains. Markedly, D01 under SSP 5-8.5, shows strong increases during most of the months in the year by the end of the century, while maintaining the October peak rainfall. The high precipitation change during this month may be attributed to the withdrawal of the summer monsoon affecting future change of climate extremes. Ha et al. (2020) [38] reported that during the month of October, the summer monsoon showed a delayed retreat in the mid- to the late-21st century, thus, this may increase precipitation extremes over the mainland SEA where D01 is located.

Sub-region D02 shows noticeable decreases during the March-May months (near-term) which is strengthened progressively during the mid-term and intensified during the far-term. The rainfall change indicates higher proportions of the Northeast Monsoon rainfall during the end of the year. This is also consistent with the downscaled projections simulations undertaken by Villafuerte et al. (2020) [39] who reported that the projected Northeast Monsoon

rainfall in the Philippines indicated a robust increase in most areas in the mid-21st century under the high-emission scenario.

While the annual rainfall changes in the near-term of sub-region D03 has a minimal increase, the increases in the mid- and far-term are apparent. The strengthening of the Northeast Monsoon rains by November-January is evident by the end of the century. These changes in the annual cycle imply strong future changes in the two main monsoon seasons (Northeast and Southwest) which influence the precipitation regime of Southeast Asia. The policy options, depending on which region is dependent on which monsoon season for rainfall, therefore need to be based on these plausible changes that are relevant to water resources management or extreme events such as floods/droughts/agricultural practices.

3.5 Low-level moisture flux convergence and its transport

Figure 6 illustrates the low-level (850hPa) moisture flux convergence (MFC) across various SSPs for the far-term period, which partially explains the wetting and drying patterns presented in **Figure 2**. The dry regions in **Figure 2** correspond to the negative MFC values, while wet regions correspond to positive MFC values. This underscores the significance of MFC in determining precipitation patterns. Furthermore, in the ANN of SSP5-8.5, there is a minimal drying in central mainland SEA, Indonesia, and south of Philippines and this is due to the moisture divergence along those regions. The projected increase in rainfall in northern Myanmar (**Figure 2**) is attributed to the moisture convergence over the Tibetan Plateau and South China.

The projected drying tendency during DJF, specifically in mainland SEA is due to the intensified northeast monsoon wind flow (**Figure S3** provides further evidence). The intensified wind flow is accompanied by a strong signal of moisture flux divergence over the ocean, which ultimately results in reduced moisture transport over the land. For the MAM season, the MFC shows minimal changes across different SSPs, and dry regions mainly result from mass divergence in mainland SEA, Sumatra, and the Philippines.

For JJA, interaction of ocean and land dynamics plays an important role specially in maritime continent but for the northern mainland SEA the projected wet regions are mainly influenced by the moisture convergence over Tibetan Plateau and minimally from the southwest monsoon. Additionally, the result suggests an intensification of the southwest monsoon in the far-term period, mainly delineating horizontal mass divergence across the SEA region (**Figure S3**). Increases in Asian monsoon precipitation is analogous to the study of Chen et al. (2020) [40] and Wang et al. (2020) [41]. Furthermore, the projected increase in summer monsoon precipitation is linked to the projected large changes on the land and ocean thermal contrast [41].

3.6 Relationship of changes in rainfall, moisture to global warming

The agreement of spatial pattern of correlation of global mean temperature and rainfall is remarkable, particularly the distinctive transition of the sign between positive and negative response in the north and south of equator during ANN, respectively (**Figure 7**). Significantly high correlations were obtained in SSP1-2.6 scenario while lower but significant correlations in a warmer climate. Seasonal correlations depict different variations in the northern latitudes but consistently a negative correlation in the south. It was reported that the atmospheric moisture is a key factor for changes in rainfall [42]. Atmospheric moisture at different scenario has a linear dependence on global warming (**Figure S4**). We found a positive correlation of moisture and GMT at 0° to 28°N which coincides with the increased in rainfall while some parts of maritime continent yield a negative correlation that coincides with decreases in rainfall at different warming scenarios.

Furthermore, we analyzed the sensitivities of SEA precipitation on global mean temperature (GMT) under different emission scenarios (**Figure 8**). Sensitivity of precipitation changes is found to have a linear dependence on the changes in GMT. We

found that the annual response rate of precipitation to GMT under SSP1-2.6 is found highest among the scenarios whereas SSP5-8.5 yielded lowest. The median precipitation rate of increase with warming is at 8.9%, 6.3%, 3.6%, and 2.7% under SSP1-2.6, 2-4.5, 3-7.0, and 5-8.5, respectively. This means that the rate of change in precipitation per degree Celsius of GMT is more sensitive in SSP1-2.6 than in higher emission scenarios. Moreover, a slight increase in GMT is likely to trigger higher changes in precipitation under SSP1-2.6. The higher climate sensitivity of SSP1-2.6 is also found by Jiang et al. (2020) [31] over the semi-arid region of Central Asia.

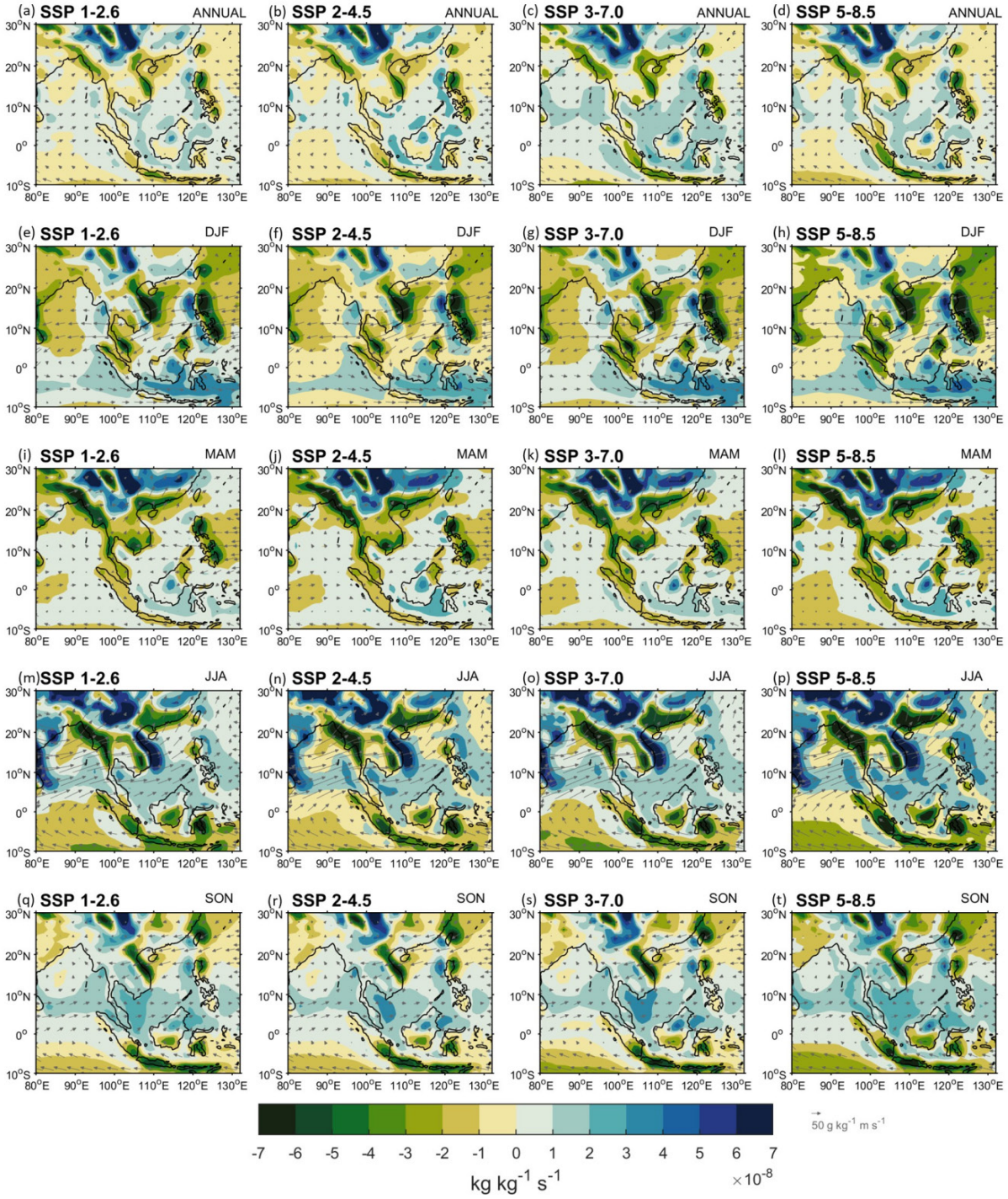

Figure 6. Low-level (850-hPa) moisture flux convergence (unit: kg kg-1 s-1) for the far-term period (2081–2100).

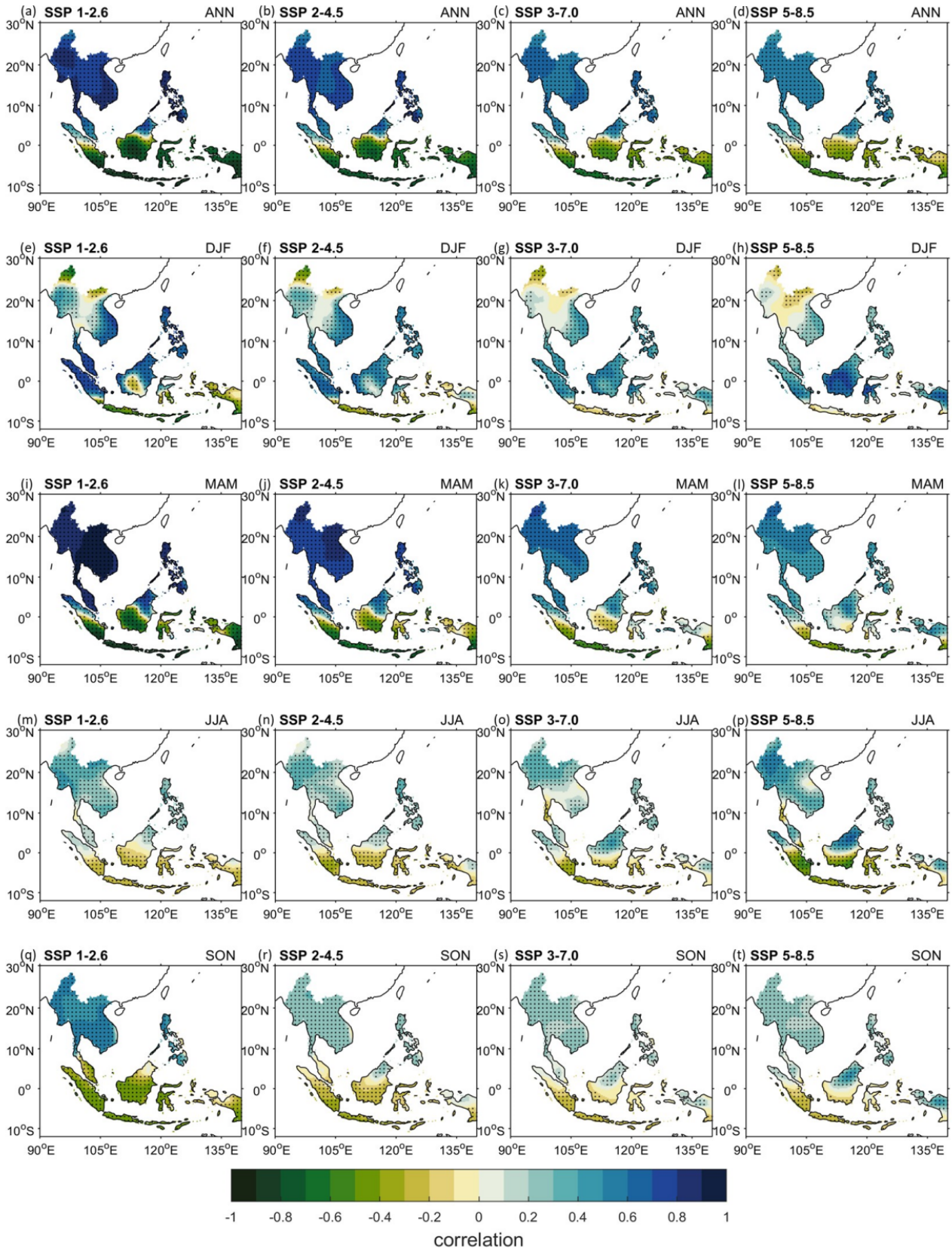

Figure 7. Spatial correlation of GMT and rainfall changes for 2021–2099. Stippling indicates 95% confidence level.

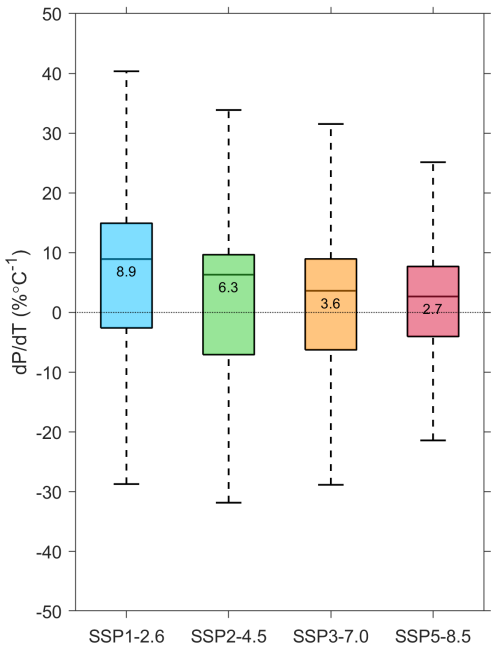

Figure 8. Responses of precipitation changes to global mean temperature changes for 2021–2099.

4. Conclusions

We analysed the future projections of rainfall using an ensemble of 48 CMIP6 models under different climate scenarios (SSPs 1-2.6, 2-4.5, 3-7.0 and 5-8.5), over Southeast Asia. Overall, the results suggest that the end of the century is likely to experience higher magnitude of changes in rainfall compared to the near and mid-term periods. The box-plot analyses show that the future changes among models indicate a strong median increase up to 9% towards the end of the century. Possible extreme changes suggest a substantial increase of 22% (far-term of SSP 5-8.5) and a decrease of about 8% (near-term of SSP 3-7.0) as represented by the 90th and 10th percentiles, respectively. Nevertheless, the continued increase over the entire SEA is evident. The future changes in the annual cycles of rainfall are suggestive of the changes that are likely to be brought in by the two main monsoon seasons (Northeast and Southwest) which influence the precipitation regime of Southeast Asia. The study highlights the significance of MFC in determining the precipitation patterns and dry and wet tendencies across different seasons and regions. The results suggest that MFC plays a crucial role in the projected increase and decrease of rainfall in SEA regions.

Generally, in an annual scale, higher increases (decreases) in rainfall over north (south) of equator is attributed to GMT. In addition, future change in rainfall under different scenario and GMT is found to have linear responses. The precipitation rate of increase with warming is at 8.9%, 6.3%, 3.6%, and 2.7% under SSP1-2.6, 2-4.5, 3-7.0, and 5-8.5, respectively. The policy options, depending on which region is dependent on which monsoon season for rainfall, therefore need to be based on these plausible changes that are relevant to water resources management or extreme events such as floods/droughts/agricultural practices.

Whilst climate projection uncertainties are intrinsic from global climate model simulations, the results indicate the need for better representation of the earth system in these models. Tangang et al. (2020) [10] noted that downscaling the GCMs to a higher spatial resolution (<25 km) would lead to the intrinsic improvement of their systematic errors and uncertainties. The results related to the changes in rainfall are not much different from the CMIP5 suite of models and especially the changes to extremes need further quantification when all the analyses can be revisited using daily scale data. Precipitation extremes are not well-represented in CMIP6 models but improved from CMIP5 to CMIP6 models [7,20]. However, these initial results do offer useful information to policy makers to obtain a reasonable understanding of possible changes to come though limitations and uncertainties exist in the model dynamics and as well as in better quantification of the magnitudes of these changes. O'Neill et al. (2016) [35] noted that the scenario-based CMIP6 models (SSPs) would facilitate wide range of scientifically guided policies that are relevant on the effect of the increase or decrease of climate forcing in the models. Despite weaknesses and uncertainty in the CMIP6 models, broad consistency between models provides high confidence in understanding future changes which could be studied further as newer data become available to the research community.

Author contributions

BO and SR conceptualized the study. BO worked out most of the technical details, analytic calculations, and visualization. BO and SR wrote the manuscript with input from all authors. NN, SN, and TN contributed to the final version of the manuscript. All authors provided critical feedback and helped shape the research, analysis, and manuscript.

Conflict of Interest

The authors declare that they have no conflict of interest.

Data Availability Statement

The data used in this study are obtained from the Coupled Model Intercomparison Project Phase 6 (CMIP6) archive. All CMIP6 model output used in this research is publicly available through the Earth System Grid Federation (ESGF) nodes. For further information on data access and usage policies refer to the CMIP6 data portal (https://esgf-node.llnl.gov/projects/cmip6/)

Funding

The authors declare that no funds, grants, or other support were received during the preparation of this manuscript.

Acknowledgments

We would like to express our sincere gratitude to the anonymous reviewers for their insightful comments, constructive feedback, and thorough review of this manuscript. Their expertise and dedication greatly contributed to improving the quality and clarity of our work. We appreciate their time and effort invested in evaluating our research and guiding its development.

References

[1] Intergovernmental Panel on Climate Change (IPCC), 2023. Climate change 2021-The physical science basis: Working group I contribution to the sixth assessment report of the intergovernmental panel on climate change. Cambridge University Press: Cambridge, UK and New York, NY, USA. pp. 1–2392.
DOI: https://doi.org/10.1017/9781009157896

[2] Intergovernmental Panel on Climate Change (IPCC), 2023. Climate change 2022-Impacts, adaptation and vulnerability: Working group II contribution to the sixth assessment report of the intergovernmental panel on climate change. Cambridge University Press: Cambridge, UK and New York, NY, USA. pp. 1–3056.
DOI: https://doi.org/10.1017/9781009325844

[3] Intergovernmental Panel on Climate Change (IPCC), 2023. Climate Change 2022-Mitigation of Climate Change: Working Group III Contribution to the Sixth Assessment Report of the Intergovernmental Panel on Climate Change. Cambridge University Press: Cambridge, UK and New York, NY, USA. pp. 1–2030.
DOI: https://doi.org/10.1017/9781009157926

[4] Eyring, V., Bony, S., Meehl, G.A., et al, 2016. Overview of the coupled model intercomparison project phase 6 (CMIP6) experimental design and organization. Geoscientific Model Development. 9(5), 1937–1958.
DOI: https://doi.org/10.5194/gmd-9-1937-2016

[5] Cook, B.I, Mankin, J.S, Marve, K., et al, 2020. Twenty-First century drought projections in the CMIP6 forcing scenarios. Earth' s Future. 8(6), 1–20.
DOI: https://doi.org/10.1029/2019EF001461

[6] Li, C., Zwiers, F., Zhang, X., et al, 2021. Changes in annual extremes of daily temperature and precipitation in CMIP6 models. Journal of Climate. 34(9), 3441–3460.
DOI: https://doi.org/10.1175/jcli-d-19-1013.1

[7] Scoccimarro, E., Gualdi, S., 2020. Heavy daily precipitation events in the CMIP6 worst-case scenario: Projected twenty-first-century changes. Journal of Climate. 34(17), 7631–7642.

DOI: https://doi.org/10.1175/JCLI-D-19-0940.1

[8] Ukkola, A.M, De Kauwe, M.G, Roderick, M.L, et al., 2020. Robust future changes in meteorological drought in CMIP6 projections despite uncertainty in precipitation. Geophysical Research Letters. 47(11), 1–9.
DOI: https://doi.org/10.1029/2020GL087820

[9] Hijioka, Y., Lasco, R., Surjan, A., et al., 2014. Climate change 2014: impacts, adaptation, and vulnerability. Part B Regional aspects. Contribution of working group II to the Fifth Assessment Report of the IPCC. Cambridge University Press: Cambridge, UK. pp. 1–1820.
DOI: https://doi.org/10.1017/CBO9781107415386

[10] Tangang, F., Chung, J.X., Juneng, L., et al., 2020. Projected future changes in rainfall in southeast Asia based on CORDEX–SEA multi-model simulations. Climate Dynamics. 55, 1247–1267.
DOI: https://doi.org/10.1007/s00382-020-05322-2

[11] Villafuerte, M.Q., Matsumoto, J., 2015. Significant influences of global mean temperature and ENSO on extreme rainfall in Southeast Asia. Journal of Climate. 28(5), 1905–1919.
DOI: https://doi.org/10.1175/JCLI-D-14-00531.1

[12] Arnell, N.W., Lowe, J.A., Lloyd-Hughes, B., et al., 2018. The impacts avoided with a 1.5 ºC climate target: a global and regional assessment. Climatic Change. 147, 61–76.
DOI: https://doi.org/10.1007/s10584-017-2115-9

[13] Brown, S., Nicholls, R.J., Lowe, J.A., et al., 2016. Spatial variations of sea-level rise and impacts: An application of DIVA. Climatic Change. 134, 403–416.
DOI: https://doi.org/10.1007/s10584-013-0925-y

[14] Hinkel, J., Lincke, D., Vafeidis, A.T., et al., 2014. Coastal flood damage and adaptation costs under 21st century sea-level rise. Pnas. 111(9), 3292–3297.
DOI: https://doi.org/10.1073/pnas.1222469111

[15] Hoegh-Guldberg, O., Jacob, D., Taylor, M., et al., 2018. Impacts of 1.5 °C global warming on natural and human systems. In: Global Warming of 1.5 °C. An IPCC Special Report on the impacts of global warming of 1.5 ºC above pre-industrial levels and related global greenhouse gas emission pathways, in the context of strengthening the global response to the threat of climate change, sustainable development, and efforts to eradicate poverty. IPCC. Cambridge University Press: Cambridge, UK and New York, NY, USA. pp. 175–312.
DOI: https://www.ipcc.ch/sr15/chapter/chapter-3/

[16] Liu, W., Sun, F., Lim, W.H., et al, 2018. Global drought and severe drought-affected populations in 1.5 and 2 °C warmer worlds. Earth System Dynamics. 9(1), 267–283.
DOI: https://doi.org/10.5194/esd-9-267-2018

[17] Schleussner, C., Lissner, T.K., Fischer, E.M., et al., 2016. Differential climate impacts for policy-relevant limits to global warming : the case of 1.5 ºC and 2 ºC. Earth System Dynamics. 7(2), 327–351.
DOI: https://doi.org/10.5194/esd-7-327-2016

[18] Settele, J., Scholes, R., Africa, S., et al., 2014. Terrestrial and Inland Water Systems. In: Climate Change 2014: Impacts, Adaptation, and Vulnerability. Part A: Global and Sectoral Aspects. Contribution of Working Group II to the Fifth Assessment Report of the Intergovernmental Panel on Climate Change. Cambridge University Press: Cambridge, UK and New York, NY, USA, pp. 271–359.

[19] Chen, H., Sun, J., 2018. Projected changes in climate extremes in China in a 1.5 °C warmer world. International Journal of Climatology. 38(9), 3607–3617.
DOI: https://doi.org/10.1002/joc.5521

[20] Chen, C.A., Hsu, H.H., Liang, H.C., 2021. Evaluation and comparison of CMIP6 and CMIP5 model performance in simulating the seasonal extreme precipitation in the Western North Pacific and East Asia. Weather and Climate Extremes. 31, 100303.
DOI: https://doi.org/10.1016/j.wace.2021.100303

[21] Nikulin, G., Lennard, C., Dosio, A., et al., 2018. The effects of 1.5 and 2 degrees of global warming on Africa in the CORDEX ensemble.

Environmental Research Letters. 13, 65003.
DOI: https://doi.org/10.1088/1748-9326/aab1b1

[22] Ge, F., Zhu, S., Luo, H., et al, 2021. Future changes in precipitation extremes over Southeast Asia: Insights from CMIP6 multi-model ensemble. Environmental Research Letters. 16, 024013.
DOI: https://doi.org/10.1088/1748-9326/abd7ad

[23] Huang, W.R., Chang, Y.H., Deng, L., et al, 2021. Simulation and projection of summer convective afternoon rainfall activities over southeast Asia in CMIP6 models. Journal of Climate. 34(12), 1–43.
DOI: https://doi.org/10.1175/JCLI-D-20-0788.1

[24] Sillman, J., Stjern, C.W., Myhre, G., Forster, P., 2017. Slow and fast responses of mean and extreme precipitation to different forcing in CMIP5 simulations. Geophysical Research Letters. 44(12), 6383–6390.
DOI: https://doi.org/10.1002/2017GL073229

[25] Sillmann, J., Kharin, V.V., Zwiers, F.W., et al., 2013. Climate extremes indices in the CMIP5 multimodel ensemble: Part 2. Future climate projections. Journal of Geophysical Research: Atmospheres. 118(6), 2473–2493.
DOI: https://doi.org/10.1002/jgrd.50188

[26] Almazroui, M., Islam, M.N., Saeed, F., et al., 2021. Projected changes in temperature and precipitation over the United States, central America, and the Caribbean in CMIP6 GCMs. Earth Systems and Environment. 5, 1–24.
DOI: https://doi.org/10.1007/s41748-021-00199-5

[27] Almazroui, M., Saeed, F., Saeed, S., et al., 2020. Projected change in temperature and precipitation over Africa from CMIP6. Earth Systems and Environment. 4, 455–475.
DOI: https://doi.org/10.1007/s41748-020-00161-x

[28] Almazroui, M., Saeed, S., Saeed, F., et al., 2020. Projections of precipitation and temperature over the South Asian Countries in CMIP6. Earth Systems and Environment. 4, 297–320.
DOI: https://doi.org/10.1007/s41748-020-00157-7

[29] Dantas, L.G., dos Santos C.A.C., Santos, C.A.G., et al, 2022. Future changes in temperature and precipitation over Northeastern Brazil by CMIP6 model. Water. 14(24), 4118.
DOI: https://doi.org/10.3390/w14244118

[30] Gupta, V., Singh, V., Jain, M.K., 2020. Assessment of precipitation extremes in India during the 21st century under SSP1-1.9 mitigation scenarios of CMIP6 GCMs. Journal of Hydrology. 590, 125422.
DOI: https://doi.org/10.1016/j.jhydrol.2020.125422

[31] Jiang, J., Zhou, T., Chen, X., et al., 2020. Future changes in precipitation over Central Asia based on CMIP6 projections. Environmental Research Letters. 15, 054009.
DOI: https://doi.org/10.1088/1748-9326/ab7d03

[32] Mesgari, E., Hosseini, S.A., Hemmesy, M.S., et al, 2022. Assessment of CMIP6 models' performances and projection of precipitation based on SSP scenarios over the MENAP region. Journal of Water & Climate Change.13(10), 3607–3619.
DOI: https://doi.org/10.2166/wcc.2022.195

[33] Moradian, S., Torabi Haghighi, A., Asadi, M., et al., 2023. Future changes in precipitation over Northern Europe based on a multi-model ensemble from CMIP6: Focus on Tana River Basin. Water Resources Management. 37, 2447–2463.
DOI: https://doi.org/10.1007/s11269-022-03272-4

[34] Zhai, J., Mondal, S.K., Fischer, T., et al., 2020. Future drought characteristics through a multi-model ensemble from CMIP6 over South Asia. Atmospheric Research. 246, 105111.
DOI: https://doi.org/10.1016/j.atmosres.2020.105111

[35] O'Neill, B.C., Tebaldi, C., van Vuuren, D.P., et al., 2016. The scenario model intercomparison project (ScenarioMIP) for CMIP6. Geoscientific Model Development. 9(9), 3461–3482.
DOI: https://doi.org/10.5194/gmd-9-3461-2016

[36] Banacos, P. C., Schultz, D. M., 2005. The use of moisture flux convergence in forecasting convective initiation: historical and operational perspectives. Weather and Forecasting. 20(3), 351–366.
DOI: https://doi.org/10.1175/WAF858.1

[37] Tian. B., Dong, X., 2020. The double-ITCZ bias in CMIP3, CMIP5, and CMIP6 models based on annual mean precipitation. Geophysical Research Letters. 47(8), 1–11. DOI: https://doi.org/10.1029/2020GL087232

[38] Ha, K.J., Moon, S., Timmermann, A., et al., 2020. Future changes of summer Monsoon characteristics and evaporative demand over Asia in CMIP6 simulations. Geophysical Research Letters. 47(8), 1–10. DOI: https://doi.org/10.1029/2020GL087492

[39] Villafuerte, M.Q., Macadam, I., Daron, J., et al., 2020. Projected changes in rainfall and temperature over the Philippines from multiple dynamical downscaling models. International Journal of Climatology. 40(3), 1784–1804. DOI: https://doi.org/10.1002/joc.6301

[40] Chen, Z., Zhou, T., Zhang, L., et al., 2020. Global land monsoon precipitation changes in CMIP6 projections. Geophysical Research Letters. 47(14), 1–9. DOI: https://doi.org/10.1029/2019GL086902

[41] Wang, B., Jin, C., Liu, J., 2020. Understanding future change of global monsoons projected by CMIP6 models. Journal of Climate. 33(15), 6471–6489. DOI: https://doi.org/10.1175/JCLI-D-19-0993.1

[42] Moon, S., Ha, K.J., 2020. Future changes in monsoon duration and precipitation using CMIP6. npj Climate Atmospheric Science. 3, 1–7. DOI: https://doi.org/10.1038/s41612-020-00151-w

Appendix

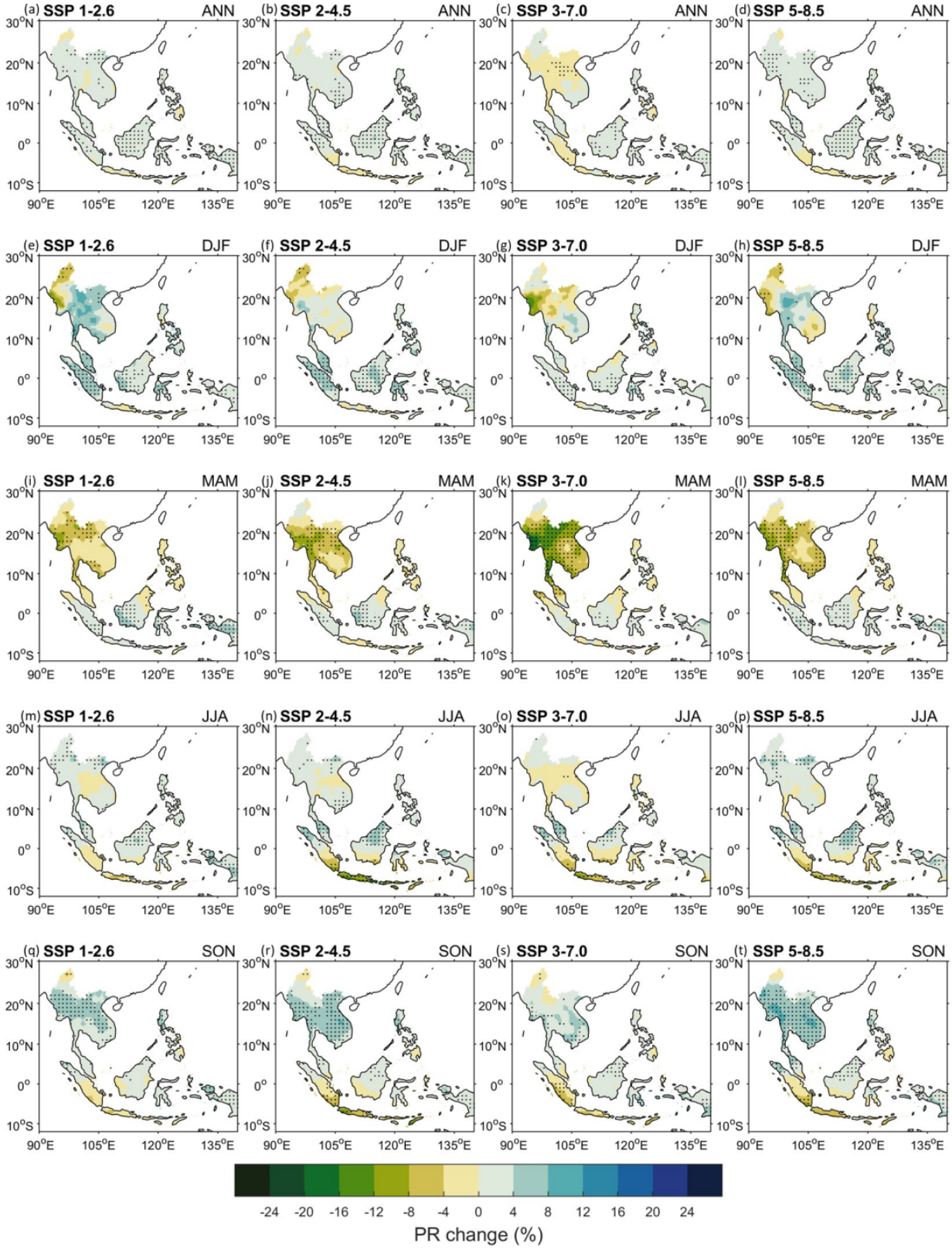

Figure S1. Spatial distribution of (**a–d**) annual and (**e–t**) seasonal precipitation changes for the near-term (2021–2040). Stippling indicates that at least two-thirds of the models agree on the sign of changes.

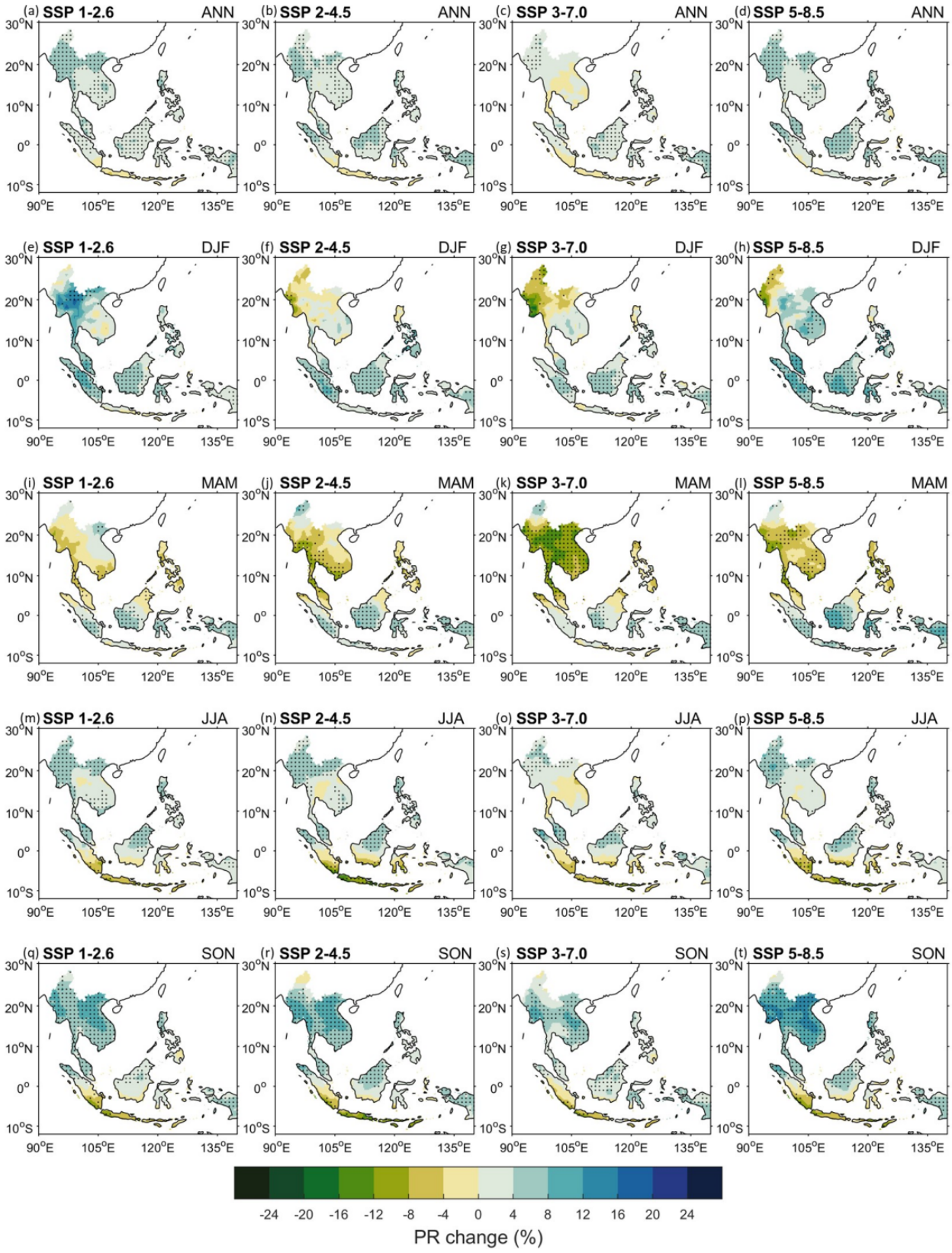

Figure S2. Spatial distribution of (**a–d**) annual and (**e–t**) seasonal precipitation changes for the mid-term (2041–2060). Stippling indicates that at least two-thirds of the models agree on the sign of changes.

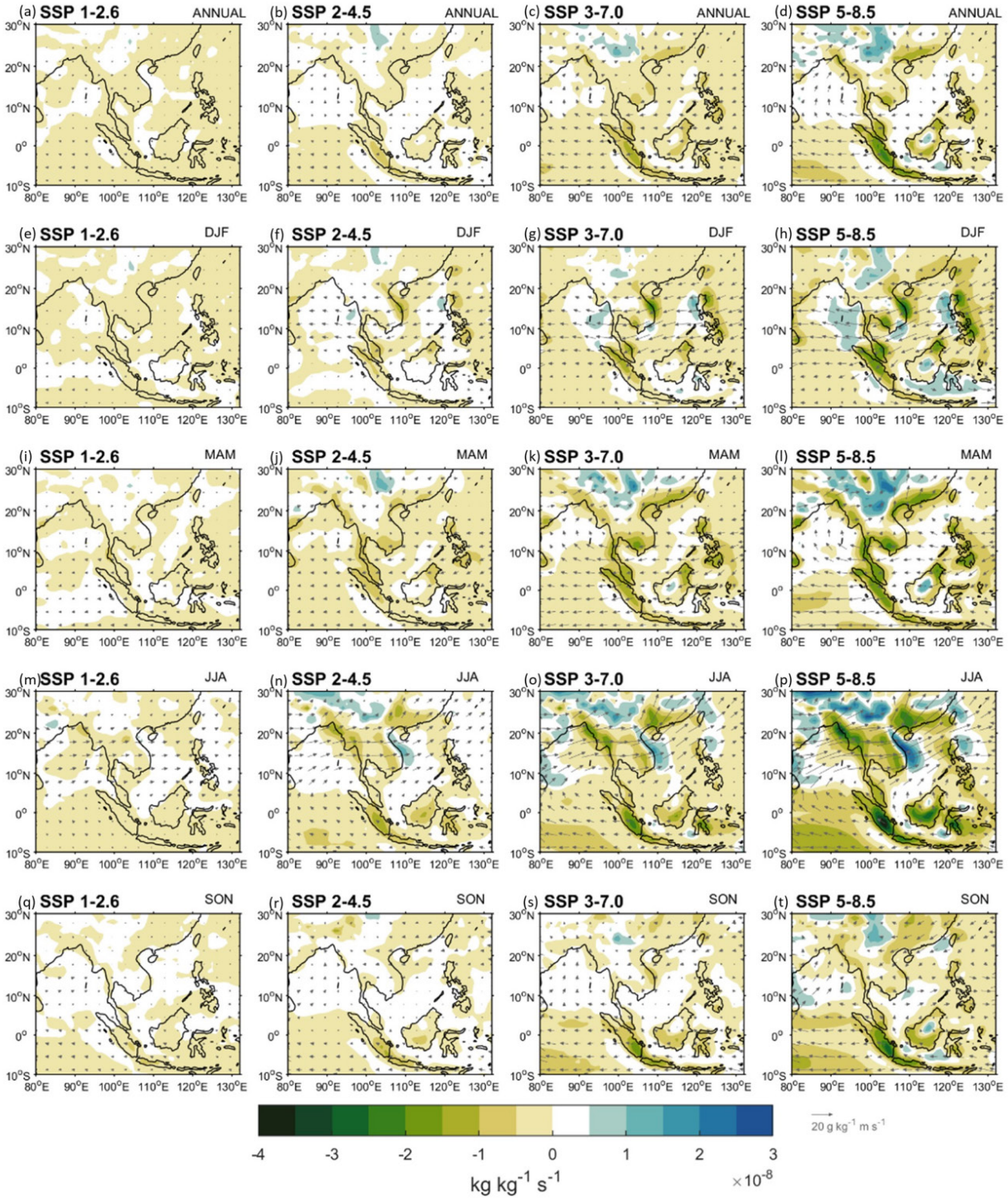

Figure S3. Low-level (850hPa) moisture flux convergence difference of far-term and near-term. The difference of far-term and near-term highlights the moisture flux suppression and intensification across different seasons.

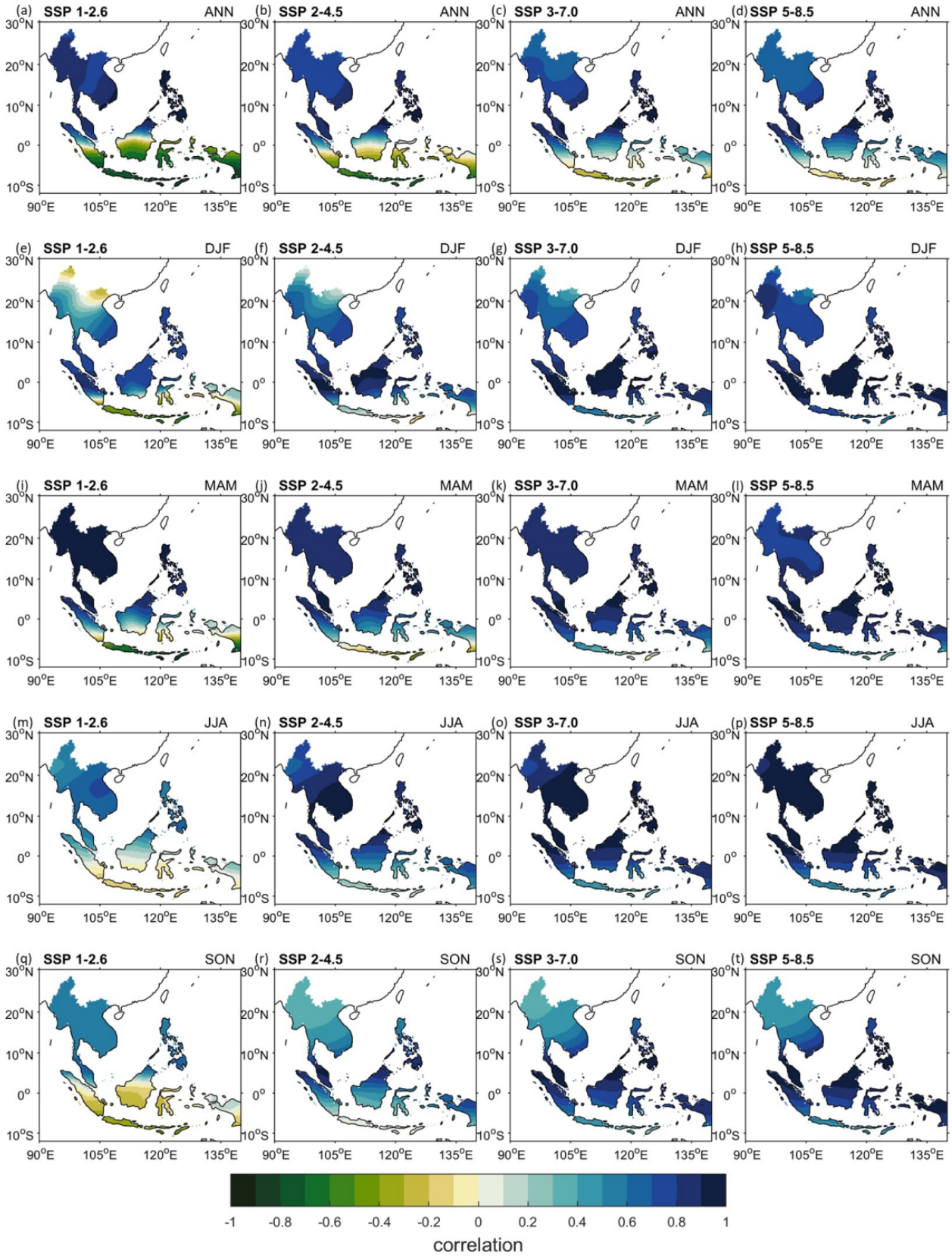

Figure S4. Spatial correlation of GMT and atmospheric moisture for 2021–2099. Stippling indicates 95% confidence level.